Volume 55
Number 8
24 February 2026
Pages 3155-3588

Dalton Transactions

An international journal of inorganic chemistry

rsc.li/dalton

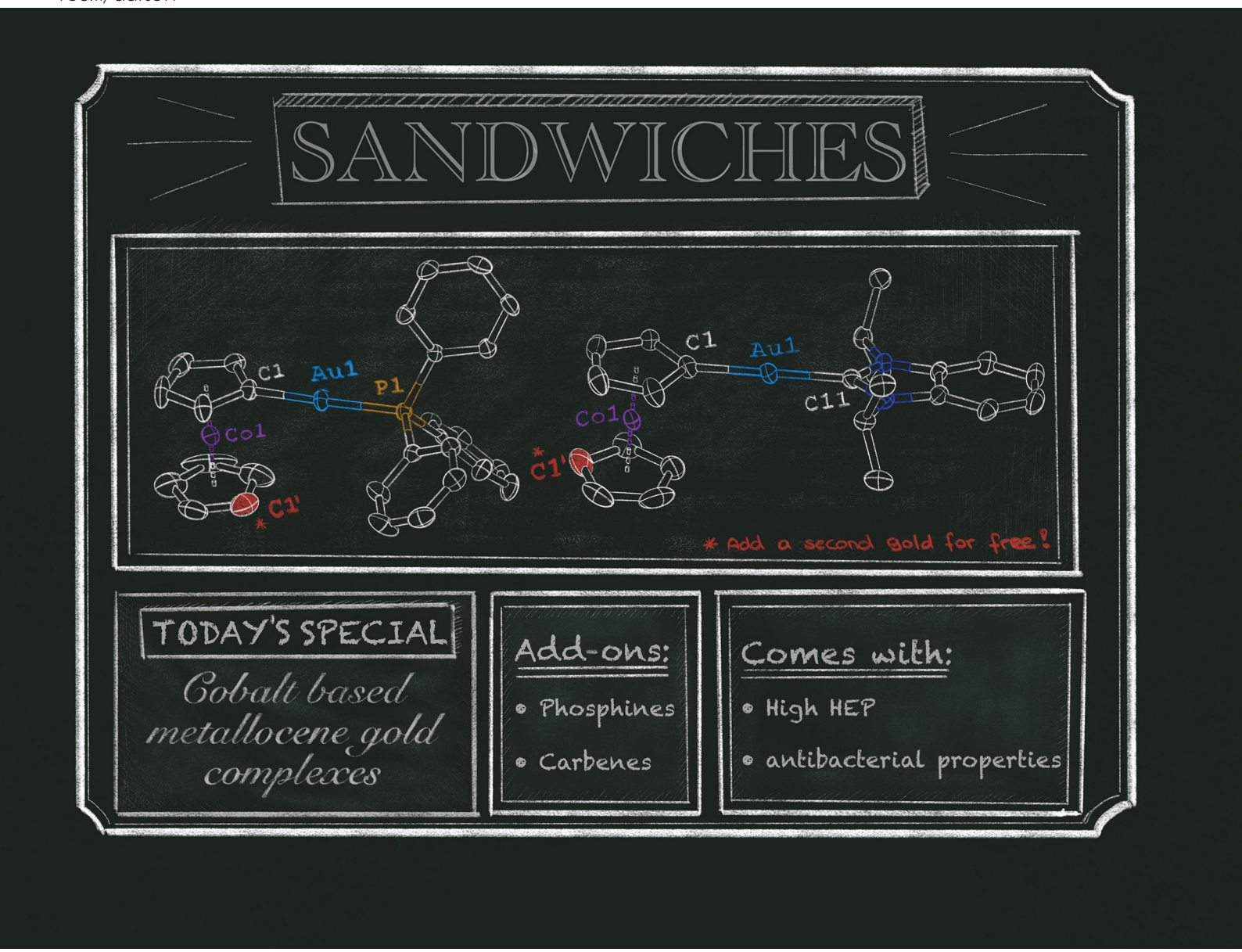

ISSN 1477-9226

ROYAL SOCIETY OF CHEMISTRY

PAPER
Stephan Hohloch *et al.*
Cobalt-based metallo-mesoionic carbene gold complexes with antiproliferative effects

Dalton Transactions

PAPER

View Article Online
View Journal | View Issue

Check for updates

Cite this: *Dalton Trans.*, 2026, **55**, 3259

Cobalt-based metallo-mesoionic carbene gold complexes with antiproliferative effects

D. Menia, [a] F. R. Neururer, [a] K. Wurst,[a] P. Lippmann,[b] I. V. Esarev,[b] M. Seidl,[a] I. Ott, *[b] M. Podewitz, *[c] S. Hohloch *[a] and B. Bildstein *[a]

Received 23rd October 2025,
Accepted 2nd December 2025

DOI: 10.1039/d5dt02549d

rsc.li/dalton

We report the facile synthesis of new gold(I) carbene complexes based on a mesoionic cobaltocenylidene metallocarbene *via* a fluorinative desilylation reaction. The carbene has been characterized by a variety of spectroscopic methods, revealing that it has the highest HEP value reported for a MIC so far, suggesting that the carbene is highly electron donating. The properties of the new class of metallo-mesoionic carbenes is further investigated, revealing also exceptionally low TEP values. Electrochemical studies also suggest the cobaltocenium moiety to be further reducible. In addition, the cell growth inhibitory effects of the new metallocarbene complexes were explored in cancer cells and bacteria. The combination of electrochemical activity, exceptional electron donating properties and their putative application in medicinal chemistry makes these new metallo-MICs a highly interesting new class of ligands.

Open Access Article. Published on 17 December 2025. Downloaded on 6/10/2026 11:02:15 PM.
This article is licensed under a Creative Commons Attribution 3.0 Unported Licence.

Introduction

Undoubtedly, few ligand families have changed the chemical landscape as much as N-heterocyclic carbenes (NHCs).[1,2] Since their first exploration by Wanzlick and Öfele[3] and the subsequent isolation of the first free carbenes,[4] NHCs have played a crucial role in the development and application of organometallic chemistry.[1,2,5] It is therefore no surprise that over recent decades a plethora of subclasses have emerged, ranging from classical *n*NHCs to remote NHCs[6,7] and cyclic alkyl/aryl-(amino) carbenes[8] to abnormal or mesoionic carbenes.[6,7,9–12] In particular, during the past two decades, the latter have emerged from laboratory curiosities to a valuable and important subclass of NHCs.[7,9,13] This is partly related to the development of mesoionic carbenes (MICs) based on ubiquitously accessible triazoles (so-called triazolylidenes)[9–11,13] as well as their unique electronic properties rating them as strongly electron donating carbenes. Given the modular approach of NHC synthesis, the donating abilities of the NHC ligands can be tuned quite easily. However, this approach requires the synthesis of new ligands, changing in most cases also the steric properties of the flanking groups. Thus, redox-active NHCs have emerged in the literature.[14–16] These allow the tuning of the electronic structure of the NHC/MIC ligand by simple oxidation/reduction without the need for tedious synthetic remodeling. This has been achieved by either the introduction of redox-active groups into the backbone of the ligand (*e.g.* chinones or ferrocenes)[14,16] or the introduction of redox-active wingtip groups, in most cases ferrocene or cobaltocene(ium) groups.[17] However, in all these cases, the redox-active group is not an integral part of the NHC framework but covalently linked to it. In contrast to this, in 2018, we reported the synthesis of a purely metallocene-based mesoionic carbene termed 1-cobaltocenylidene **1a′** with a gold(III) central metal.[18] This carbene differs from previous redox-active carbenes because the carbene carbon is directly part of the redox-active group. However, the original synthesis lacked variability and only 1-cobaltocenylidene was accessible *via* this route while 1,1′-cobaltocenylidene was not.[18] Furthermore, the reaction only proceeded from the 1-diazoniumcobaltocenium bis-hexafluorophosphate di-cation, which is tedious to prepare in a four-step synthesis and can only be stored for a prolonged time at low temperatures.[19] Ultimately, the reaction starts from a gold(I) source, but a gold(III) complex is finally isolated. Thus, we aimed to expand the synthesis to a more versatile and direct approach. Herein, we demonstrate the simple synthetic accessibility of 1-cobaltocenylidene and 1,1′-cobaltocenylidene making use of a fluorinative desilylation reaction starting from readily accessible 1,1′-trimethylsilylcobaltocenium

[a]*Department of General, Inorganic and Theoretical Chemistry, University of Innsbruck, Innrain 80–82, 6020 Innsbruck, Austria. E-mail: Stephan.Hohloch@uibk.ac.at, Benno.Bildstein@uibk.ac.at*
[b]*Institute of Medicinal and Pharmaceutical Chemistry, Technische Universität Braunschweig, Beethovenstraße 55, 38106 Braunschweig, Germany. E-mail: ingo.ott@tu-braunschweig.de*
[c]*Institute of Materials Chemistry, Technische Universität Wien, Getreidemarkt 9, 1060 Wien, Austria. E-mail: maren.podewitz@tuwien.ac.at*

Open Access Article. Published on 17 December 2025. Downloaded on 6/10/2026 11:02:15 PM. This article is licensed under a Creative Commons Attribution 3.0 Unported Licence.

hexafluorophosphate **1**.[20] A library of gold(I) complexes is reported and their respective redox, electronic and antiproliferative properties are explored.

Results and discussion

Starting from readily accessible bis-TMS-cobaltocenium hexafluorophosphate $[(Cp^{TMS})_2Co][PF_6]$ **1**,[20] we envisioned that in the presence of fluoride donors, C–Si bond cleavage would occur, which would allow trapping of the desired cobaltocenylidene species **2a** or **2b** using gold(I) precursors. Indeed, we found that after mixing CsF, **1** and $(PPh_3)AuCl$ (3 eq.) in acetonitrile, complexes **2a** and **2b** were obtained as air and moisture-stable yellow solids after chromatographic separation using an activated aluminum oxide column. Interestingly, the product distribution between **2a** and **2b** is highly dependent on the solvent. While in acetonitrile, **2a** is the main product and **2b** is a minor product, which can be isolated in 40% and 11% yields, respectively, in THF, **2b** becomes the main product and can be isolated in 45% yield, while **2a** is only accessible in yields of 20%. However, the reaction only proceeds well if 3 equivalents of $(PPh_3)AuCl$ are used, while lower amounts of the gold reagent lead to a high amount of hydrolysis with unsubstituted cobaltocenium hexafluorophosphate being the major product of the reaction. To further investigate the reaction mechanism for the formation of the desired cobaltocenylidene complexes, we performed the reaction in wet solvents, which almost exclusively led to the isolation of the protonated cobaltocenium salts. Furthermore, changing the fluoride source was also found to be detrimental to the formation of the cobaltocenylidene complexes. Thus, we propose that gold (I) in high concentration and a fluoride source of low solubility are needed to ensure that the concentration of the transient cobaltocenylidene species is as low as possible, and trapping it as rapidly as possible. However, a full mechanistic investigation of this reaction remains outstanding. Furthermore, the reaction also works with other gold(I) precursors such as $(PMe_3)AuCl$; however, chromatographic separation of the corresponding trimethylphosphine complexes **3a** and **3b** was impossible. Formation of the new cobaltocenylidene complexes **2a** and **2b** is evident from several spectroscopic features. For the successful formation of **2a** from **1**, the first indication of formation is given by the observation of an "asymmetric" spin system in which one Cp ligand is completely protonated (δ ^{1}H = 5.52 ppm) while the other retains the typical AA′BB′ coupling pattern (Fig. S1).[18] The expected *pseudo*-triplets appear at 5.76 and 5.42 ppm and are drastically shifted compared to those of **1** in which the Cp protons are overlayed to one multiplet at 5.72 ppm.[20] This coupling pattern is retained in **2b** for both Cp rings, but the signals are shifted to 5.61 and 5.32 ppm (Fig. S6). Furthermore, for both **2a** and **2b**, the typical phenyl protons are observed between 7.72 and 7.38 ppm. The presence of the triphenylphosphine moiety is also unambiguously indicated by the observation of a ^{31}P NMR resonance at 42.9 and 43.0 ppm for **2a** and **2b**, respectively (Fig. S5/S10). Although the ^{13}C carbene resonance was not directly observed *via* one-dimensional NMR spectroscopy (Fig. S2/S7), ^{1}H–^{13}C HMBC experiments showed a cross-peak at 5.76/120.0 and 5.42/120.0 ppm in **2a** (Fig. S4) and at 5.61/118.0 and 5.32/118.0 ppm in **2b** (Fig. S9), which unambiguously belong to the cobaltocenylidene carbon atom. Final proof for the successful 1- and 1,1′-metalation in **2a** and **2b** was given by X-ray diffraction analysis (Fig. 2, and S71, S72). The carbon–gold distances Au1–C1 and Au2–C10 are 2.038(3) Å in complex **2a** and 2.070(2)/2.034(2) in complex **2b**. Compared to classical gold(I) NHC complexes, such as (IPr)AuCl (C1–Au1 1.94 Å),[21] (CAAC)AuCl (C1–Au1 1.98 Å),[22] and even (MIC)AuCl (C1–Au1 1.97 Å),[23] these distances are significantly longer, but comparable to that of cationic $[(IPr)Au(PPh_3)]^+$ (2.04 Å).[24] The P1–Au1/P2–Au2 distances are comparable at 2.2941(8) Å in **2a** and 2.2964(5)/2.2831(6) in **2b** and similar to $[(IPr)Au(PPh_3)]^+$ (2.29 Å). The Au1–Au2 distance in **2b** is 4.047(1) Å, which rules out any direct aurophilic Au–Au interactions in the complex.[25] Although we were not able to completely separate the trimethylphosphine complexes **3a** and **3b** chromatographically from each other, unambiguous proof of their synthesis was given by X-ray diffraction analysis (Fig. S73, S74). Notably, while in **2b** a torsion angle of 57.705(2)° was found between the two gold atoms, for **3b** a torsion angle of 147.679(2)° was noted, resulting in an Au1–Au2 distance of 7.509(1) Å.

The isolation of gold(I) complexes furthermore allowed the determination of the Huynh Electronic Parameter (HEP).[26] Exchange of the triphenylphosphine ligands in **2a** and **2b** works well by simple addition of the free NHC ligands and gives access to the desired carbene complexes **4a** and **4b** in the case of NHC = BenziPr ($\mathbf{L^1}$ Scheme 1) and **5a** and **5b**, if NHC = IPr ($\mathbf{L^2}$ Scheme 1) is used. Successful ligand exchange is indicated by ^{31}P NMR spectroscopy, which no longer shows any phosphine resonance. In contrast, the ^{15}N NMR spectra show resonance at 244.8, 244.8, 244.8 and 244.9 ppm (Fig. S26, S35, S44, S50) indicative of the (benz)imidazolylidene ligands in **4a**, **4b**, **5a** and **5b**.[27] Unambiguous proof for successful phosphine–NHC exchange is the appearance of a new singlet in the ^{13}C NMR spectra of the new complexes at 193.7/194.4 ppm for **4a**/**4b** (Fig. S28/S31) and at 193.0/193.9 ppm for **5a**/**5b** (Fig. S40/S46), respectively. Using the formula recently reported by Huynh ([Pd] = 1.19[Au] − 45, with [Pd] and [Au] = chemical shift of the carbene resonance in ppm),[28] the HEPs of **4a** and **4b** can be calculated to be 185.5 and 186.3 ppm, values that even exceed the highest HEP value of **Pyry-C** (Fig. 4),[29] which was reported at 184.0 ppm, making **1a**′ and $\mathbf{[1b']^-}$ (see Fig. 1 or Fig. 4 for their structures) the most strongly donating MIC ligands reported so far.[30] To place these values in more context, the HEP values of typical 2-imidazolylidenes, such as IPr, IMes, substituted benzimidazolylidenes and imidazolidines, appear in the range of 180.1–176.6 ppm, while HEPs of triazolylidenes (MIC) have been reported between 181.2 ppm and 179.5 ppm and even the more strongly donating 4-imidazolylidenes exhibit HEP values around 181.9 ppm. Thus, the new 1- and 1,1′-cobaltocenylidenes belong to the most strongly donating MICs reported so far and have (based

 This journal is © The Royal Society of Chemistry 2026

Open Access Article. Published on 17 December 2025. Downloaded on 6/10/2026 11:02:15 PM. This article is licensed under a Creative Commons Attribution 3.0 Unported Licence.

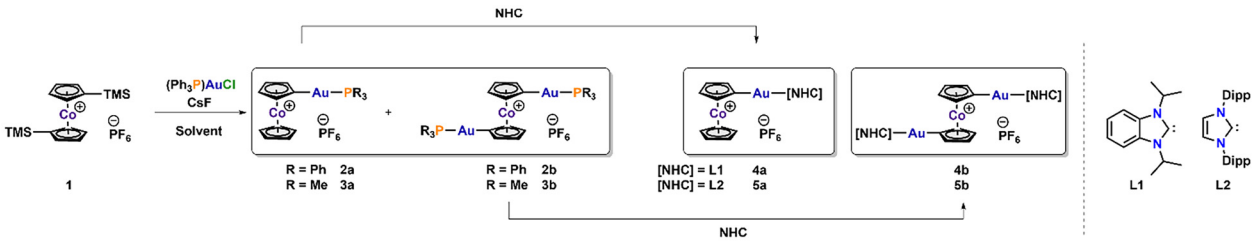

Scheme 1 Synthetic procedure towards monometallic and bimetallic 1- and 1,1′-metallated cobaltocenylidene complexes of gold(I).

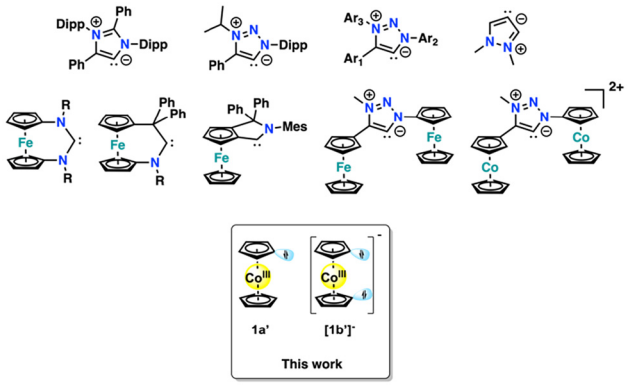

Fig. 1 Selected overview of mesoionic carbenes (first row) and metallo-NHC/MIC ligands (middle row) known in the literature compared to the examples reported here. The first three examples of the first row correspond to ligands that are known to also exist in their free form.

on their HEP values) similar donor properties compared to Dielmann's electron-rich phosphines.[31] The results from the HEP analysis are also in line with the calculated TEP parameters of the cobaltocenylidene moiety being 2037.1 cm^{-1} for the 1-cobaltocenylidene ligand **1a′**[18] and 1996.8 cm^{-1} for each carbene carbon of the 1,1′-cobaltocenylidene **[1b′]**$^-$. The X-ray structures of the complexes **4a**, **4b**, **5a** and **5b** show the expected linear coordination geometries for gold(I) NHC/MIC complexes (Fig. 2 for **4a** and **4b**; Fig. S77 (**5a**) and S78 (**5b**)). The gold–cobaltocenylidene distances Au1–C1 and Au1–C10 are similar to those of the phosphine complexes **2,3a** and **2,3b** (*vide supra*) in the range between 2.016(6) Å and 2.025(3) Å, while those of the gold (benz)imidazolylidene ligands lie in between 2.022(2) Å and 2.041(6) Å and are comparable to those of $[(IPr)Au(PPh_3)]^+$.[24] Given the redox-active nature of the cobaltocene(ylidene) moiety, we were further interested in their electrochemical properties. The phosphine complexes **2a** and **2b** show a reversible one-electron reduction at −1.55 and −1.82 V *vs.* Fc/$[Fc]^+$ (Fig. S65 and S68), while the NHC congeners **4a,b** and **5a,b** exhibit reduction potentials of −1.68, −2.05, −1.75 and −2.05 V *vs.* Fc/$[Fc]^+$. The lower reduction potentials of the NHC complexes **4** and **5** compared to **2** are in line with the higher donor strengths of the NHC ligands compared to phosphines. Unfortunately, we have not been able to chemically isolate any of these reduced complexes, but the values of the reduction potentials strongly suggest a cobalt-centred reduction process (Fig. 3).[32] To further elucidate the electronic structure of the new carbenes **1a′** and **[1b′]**$^-$ (Fig. 1 and 4), we turned to computational investigations. Computational investigations with density functional theory (PBE0/def2-TZVPP/D3BJ//BP86/def2-TZVPP/D3BJ in implicit

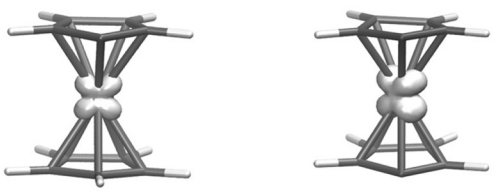

Fig. 3 Spin density calculated with the TPSSh functional for **[1a]**$^-$ and **[1b]**$^{2-}$.

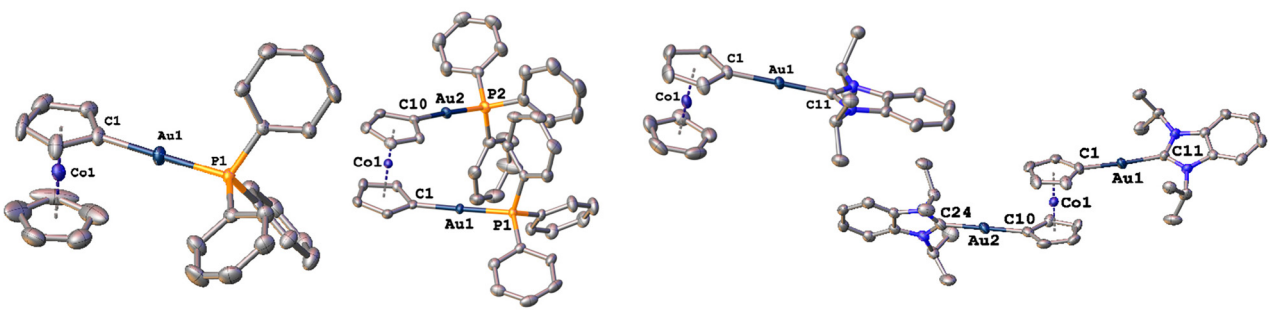

Fig. 2 Molecular structures of complex **2a**, **2b**, **4a** and **4b** (from left to right). Hydrogen atoms, counter ions and lattice solvent molecules have been omitted for clarity. Ellipsoids are shown at a probability level of 50%.

Open Access Article. Published on 17 December 2025. Downloaded on 6/10/2026 11:02:15 PM.
This article is licensed under a Creative Commons Attribution 3.0 Unported Licence.

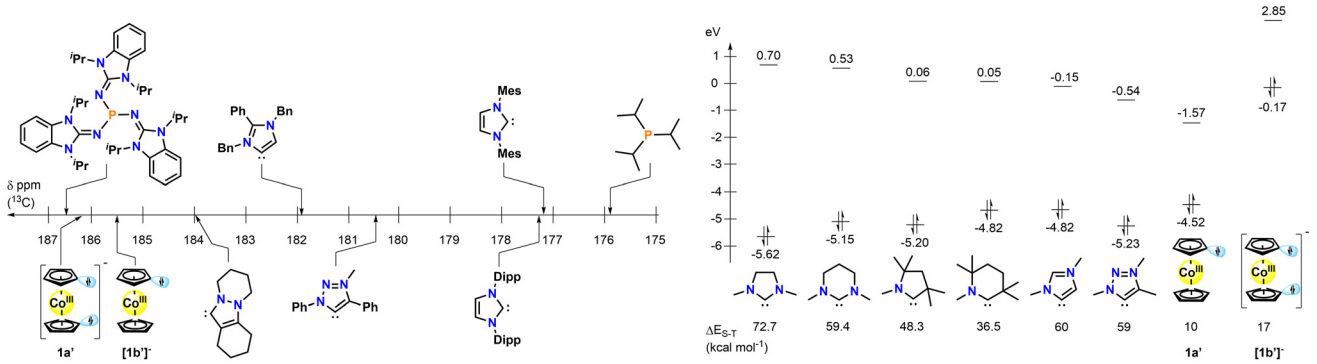

Fig. 4 Cmparison of HEP values of different NHC, MIC and phosphine donors with **1a′** and **1b′** (left) and HOMO–LUMO gaps for different NHC/ligands including the (reduced) carbenes presented here (right).

polar solvent, see the SI for details) show that both complexes **2a** and **2b** adopt a singlet state with the corresponding triplet state energies being over 100 kJ mol^{-1} higher in energy (compare Table S3 and Fig. S79 and S80). Once reduced, the ground state of the species becomes a doublet, while the energy to the quartet state is 31.5 kJ mol^{-1} (7.5 kcal mol^{-1}) and 6.7 kJ mol^{-1} (1.6 kcal mol^{-1}, Table S3). To compare these data with other (mesoionic) carbenes (see Fig. 4), the HOMO–LUMO gaps in the free carbenes were calculated with B3LYP/def2-TZVPP and were found to be 2.95 eV and 3.02 eV for the isolated ligands **1a′** and **[1b′]**$^{-}$, respectively. Calculating the singlet–triplet energy gaps in **1a′** and **[1b′]**$^{-}$ with the same methodology yields 44.0 kJ mol^{-1} (10.5 kcal mol^{-1}) and 72.2 kJ mol^{-1} (17.3 kcal mol^{-1}) in favour of the singlet state. Since the reduced complexes are not chemically accessible, we computationally determined the TEP values of the reduced cobaltocenylidene ligands. In line with the reduction of the cobalt centre (and the enhancement of the electron density at the carbene moiety), the TEPs decrease from 2037.1 cm^{-1} in **1a′** to 2015.2 cm^{-1} in **[1a′]**$^{-}$, and 1996.8 cm^{-1} (for each carbene carbon atom) in **[1b′]**$^{-}$ to 1974.8 cm^{-1} in **[1b′]**$^{2-}$. This proves that upon reduction, the cobaltocene(II)–ylidene ligands become even stronger donors and would thus belong to the most strongly donating carbenes reported so far.

Finally, we performed preliminary investigations regarding the potential of these new MIC gold(I) complexes as prospective anticancer or antibacterial drug candidates. Due to their high stability and strong effects against cancer cells, gold NHC complexes have attracted increasing interest in inorganic medicinal chemistry.[33,34] Given the fact that both gold(I) NHC[33,35] and cobaltocene(ium) supported complexes[36] have been shown to be quite potent against various tumorous and pathogenic cells,[33,37] we envisioned the new complexes to be highly active. The growth inhibitory effects of the complexes were evaluated in several tumor cell lines, a non-tumor reference cell line, and two bacterial strains (Table 1). Complexes **2a**, **2b**, and **4a–5b** generally triggered strong cytotoxic effects in MCF-7 (breast cancer), HT-29 (colon cancer) and A549 (lung cancer) cell lines with IC_{50} values in the low micromolar or sub-micromolar concentration range. Complexes **4a** and **5a** triggered stronger effects in these cancer cell lines than in the Vero-E6 non-tumor cell line (African green monkey kidney cells), which is a promising result regarding possible tumor selectivity. Interestingly, the cobaltocene derivatives with attached NHC complexes **5a** and **5b** triggered significantly stronger activity than a recently studied ferrocenyl-based NHC gold(I) complex in both cancer and non-tumor cells.[38] As for their antibacterial activity, the complexes generally exhibited very low activity or complete inactivity against the Gram-negative

Table 1 Biological results: cytotoxic effects against cancer cells (MCF-7, HT-29, and A549) and one non-tumor cell line (Vero-E6) as well as antibacterial activity against one Gram-negative (*E. coli*) and one Gram-positive (*B. subtilis*) bacterial strain

	MCF-7	HT-29	A549	Vero-E6	*E. coli*	*B. subtilis*
Ciprofloxacin·HCl	n.d.	n.d.	n.d.	n.d.	0.021 (0.003)	0.15 (0.01)
Auranofin	2.2 (0.1)	3.0 (0.8)	3.6 (0.8)	2.2 (0.6)	n.d.	n.d.
2a	4.4 (0.9)	3.8 (1.0)	3.7 (1.4)	5.8 (0.5)	>50	8.6 (1.2)
2b	1.2 (0.2)	1.9 (0.6)	1.6 (0.2)	1.8 (0.1)	>50	18.1 (0.3)
4a	0.25 (0.10)	0.48 (0.15)	0.13 (0.08)	1.58 (0.41)	>50	5.3 (1.1)
4b	0.14 (0.13)	0.12 (0.04)	0.15 (0.01)	0.13 (0.02)	21.7 (5.7)	0.26 (0.02)
5a	0.3 (0.3)	0.3 (0.3)	0.3 (0.3)	1.0 (0.1)	27.5 (4.3)	0.30 (0.03)
5b	1.8 (0.2)	2.1 (0.1)	0.6 (0.2)	5.7 (0.2)	>50	>50
5b	1.8 (0.2)	2.1 (0.1)	0.6 (0.2)	5.7 (0.2)	>50	>50

All effects are expressed as IC_{50} values and are given in μM units (± standard deviation) from 3 independent experiments or from a single experiment; ciprofloxacin and auranofin served as positive controls for antibacterial and anticancer tests, respectively.

This journal is © The Royal Society of Chemistry 2026

Open Access Article. Published on 17 December 2025. Downloaded on 6/10/2026 11:02:15 PM. This article is licensed under a Creative Commons Attribution 3.0 Unported Licence.

E. coli bacterium; however, with the exception of **5b**, all complexes demonstrated moderate to very strong activity against the Gram-positive *B. subtilis* strain. The exceptionally strong activity of **4b** and **5a** against *B. subtilis* and almost 100-fold selectivity of these two complexes in comparison with the results obtained with *E. coli* is noteworthy. Preference for Gram-positive bacteria over Gram-negative ones is a common effect of many gold compounds and can be attributed to the high sensitivity of Gram-positive bacteria towards gold-based thioredoxin reductase (TrxR) inhibitors.[33,39] For a recently reported cobaltoceniumethynyl gold(I) complex, we had confirmed strong TrxR inhibition,[40] indicating that inhibition of this essential enzyme is also a likely mechanism of action for the complexes of this report. Regarding structure–activity relationships for cytotoxic effects in cancer cells, there was a clear trend of the NHC ligands to increase bioactivity compared with the phosphine ligands. Importantly, the introduction of the cobaltocene core into the gold NHC unit tends to generally increase cytotoxic and antibacterial effects, as observed when compared to Auranofin. Thus, complex **5a** was the most active complex against the investigated tumor cells. In summary, complex **5a** emerged as the most promising compound of this study with strong and selective cell growth inhibitory effects against tumor cells as well as Gram-positive *B. subtilis*.

Conclusion

In conclusion, we have reported a versatile and simple access to new gold(I) complexes based on mesoionic 1-cobaltocenylidene and 1,1′-cobaltocenylidene carbene ligands. These carbenes were found to be among the most strongly donating MIC ligands reported so far and their donor properties can even be enhanced if the cobalt(III) centre is further reduced to cobalt(II). The biological evaluation highlighted complexes **4b** and **5a** as highly efficacious regarding their cytotoxic and Gram-positive selective antibacterial activity. Future work will focus on the implementation of these new, redox-active carbenes in switchable processes, especially in catalysis, and on further evaluating the mechanism and assessing their biological activity.

Conflicts of interest

There are no conflicts to declare.

Data availability

All data are available free of charge from our side if requested. NMRs, IR and cyclic voltammograms have been included (plotted) in the supplementary information (SI). Raw data is stored on the university servers and can be accessed *via* us if necessary. Crystallographic data (CIF-files) have been uploaded to the CCDC. Raw data and frames are stored on the university servers and can be accessed *via* us if necessary. The authors have cited additional references within the SI.[41]

Supplementary information: ^{1}H, ^{13}C, ^{31}P and 2D NMR spectra, IR and UV-Vis data as well as further information regarding X-ray crystallography and computational investigations and antiproliferative testing. See DOI: https://doi.org/10.1039/d5dt02549d.

CCDC 2314980 (**2a**), 2314979 (**2b**), 2476574 (**3b**), 2314982 (**4a**), 2314981 (**4b**), 2314983 (**5a**) and 2314984 (**5b**) contain the supplementary crystallographic data for this paper.[42a–g]

Acknowledgements

We thank the University of Innsbruck for generous funding of this work. BB and SH further acknowledge the FWF (P30221) for funding of this work.

References

1 M. N. Hopkinson, C. Richter, M. Schedler and F. Glorius, *Nature*, 2014, **510**, 485–496.
2 P. Bellotti, M. Koy, M. N. Hopkinson and F. Glorius, *Nat. Rev. Chem.*, 2021, **5**, 711–725.
3 (*a*) K. Öfele, *J. Organomet. Chem.*, 1968, **12**, P42–P43; (*b*) H.-W. Wanzlick and E. Schikora, *Angew. Chem.*, 1960, **72**, 494.
4 (*a*) A. J. Arduengo, R. L. Harlow and M. Kline, *J. Am. Chem. Soc.*, 1991, **113**, 361–363; (*b*) A. Igau, H. Grützmacher, A. Baceiredo and G. Bertrand, *J. Am. Chem. Soc.*, 1988, **110**, 6463–6466.
5 (*a*) D. Bourissou, O. Guerret, F. P. Gabbaï and G. Bertrand, *Chem. Rev.*, 2000, **100**, 39–92; (*b*) Y. K. Loh, M. Melaimi, M. Gembicky, D. Munz and G. Bertrand, *Nature*, 2023, **623**, 66–70; (*c*) D. Munz, *Organometallics*, 2018, **37**, 275–289; (*d*) S. C. Sau, P. K. Hota, S. K. Mandal, M. Soleilhavoup and G. Bertrand, *Chem. Soc. Rev.*, 2020, **49**, 1233–1252; (*e*) M. Soleilhavoup and G. Bertrand, *Chem*, 2020, **6**, 1275–1282.
6 O. Schuster, L. Yang, H. G. Raubenheimer and M. Albrecht, *Chem. Rev.*, 2009, **109**, 3445–3478.
7 R. H. Crabtree, *Coord. Chem. Rev.*, 2013, **257**, 755–766.
8 (*a*) R. Jazzar, M. Soleilhavoup and G. Bertrand, *Chem. Rev.*, 2020, **120**, 4141–4168; (*b*) M. Melaimi, R. Jazzar, M. Soleilhavoup and G. Bertrand, *Angew. Chem., Int. Ed.*, 2017, **56**, 10046–10068.
9 G. Guisado-Barrios, M. Soleilhavoup and G. Bertrand, *Acc. Chem. Res.*, 2018, **51**, 3236–3244.
10 R. Maity and B. Sarkar, *JACS Au*, 2022, **2**, 22–57.
11 W. Stroek and M. Albrecht, *Chem. Soc. Rev.*, 2024, **53**, 6322–6344.
12 Á. Vivancos, C. Segarra and M. Albrecht, *Chem. Rev.*, 2018, **118**, 9493–9586.
13 F. Gao, X. Yan and G. Bertrand, *Chem. Soc. Rev.*, 2025, **54**, 9008–9026.
14 U. Siemeling, C. Färber and C. Bruhn, *Chem. Commun.*, 2009, 98–100.

Open Access Article. Published on 17 December 2025. Downloaded on 6/10/2026 11:02:15 PM. This article is licensed under a Creative Commons Attribution 3.0 Unported Licence.

15 (*a*) A. R. Petrov, A. Derheim, J. Oetzel, M. Leibold, C. Bruhn, S. Scheerer, S. Oßwald, R. F. Winter and U. Siemeling, *Inorg. Chem.*, 2015, **54**, 6657–6670; (*b*) S. Bacaicoa, S. Stenkvist and H. Sundén, *Org. Lett.*, 2024, **26**, 3114–3118.

16 M. D. Sanderson, J. W. Kamplain and C. W. Bielawski, *J. Am. Chem. Soc.*, 2006, **128**, 16514–16515.

17 (*a*) L. Hettmanczyk, S. Manck, C. Hoyer, S. Hohloch and B. Sarkar, *Chem. Commun.*, 2015, **51**, 10949–10952; (*b*) L. Hettmanczyk, L. Suntrup, S. Klenk, C. Hoyer and B. Sarkar, *Chem. – Eur. J.*, 2017, **23**, 576–585; (*c*) S. Klenk, S. Rupf, L. Suntrup, M. van der Meer and B. Sarkar, *Organometallics*, 2017, **36**, 2026–2035; (*d*) S. Vanicek, M. Podewitz, J. Stubbe, D. Schulze, H. Kopacka, K. Wurst, T. Müller, P. Lippmann, S. Haslinger, H. Schottenberger, K. R. Liedl, I. Ott, B. Sarkar and B. Bildstein, *Chem. – Eur. J.*, 2018, **24**, 3742–3753.

18 S. Vanicek, M. Podewitz, C. Hassenrück, M. Pittracher, H. Kopacka, K. Wurst, T. Müller, K. R. Liedl, R. F. Winter and B. Bildstein, *Chem. – Eur. J.*, 2018, **24**, 3165–3169.

19 S. Vanicek, H. Kopacka, K. Wurst, T. Müller, C. Hassenrück, R. F. Winter and B. Bildstein, *Organometallics*, 2016, **35**, 2101–2109.

20 J. K. Pagano, E. C. Sylvester, E. P. Warnick, W. G. Dougherty, N. A. Piro, W. S. Kassel and C. Nataro, *J. Organomet. Chem.*, 2014, **750**, 107–111.

21 M. R. Fructos, T. R. Belderrain, P. de Frémont, N. M. Scott, S. P. Nolan, M. M. Díaz-Requejo and P. J. Pérez, *Angew. Chem., Int. Ed.*, 2005, **44**, 5284–5288.

22 V. Lavallo, G. D. Frey, S. Kousar, B. Donnadieu and G. Bertrand, *Proc. Natl. Acad. Sci. U. S. A.*, 2007, **104**, 13569–13573.

23 (*a*) L. Hettmanczyk, S. J. P. Spall, S. Klenk, M. van der Meer, S. Hohloch, J. A. Weinstein and B. Sarkar, *Eur. J. Inorg. Chem.*, 2017, **2017**, 2112–2121; (*b*) M. Rigo, L. Hettmanczyk, F. J. L. Heutz, S. Hohloch, M. Lutz, B. Sarkar and C. Müller, *Dalton Trans.*, 2016, **46**, 86–95.

24 S. Gaillard, P. Nun, A. M. Z. Slawin and S. P. Nolan, *Organometallics*, 2010, **29**, 5402–5408.

25 (*a*) H. Schmidbaur and A. Schier, *Chem. Soc. Rev.*, 2008, **37**, 1931–1951; (*b*) H. Schmidbaur and A. Schier, *Chem. Soc. Rev.*, 2012, **41**, 370–412.

26 H. V. Huynh, *Chem. Lett.*, 2021, **50**, 1831–1841.

27 (*a*) M. Baltrun, F. A. Watt, R. Schoch and S. Hohloch, *Organometallics*, 2019, **38**, 3719–3729; (*b*) F. R. Neururer, K. Huter, M. Seidl and S. Hohloch, *ACS Org. Inorg. Au*, 2023, **3**, 59–71; (*c*) F. R. Neururer, D. Leitner, S. Liu, K. Wurst, H. Kopacka, M. Seidl and S. Hohloch, *Eur. J. Inorg. Chem.*, 2023, **26**, e202300180; (*d*) F. R. Neururer, S. Liu, D. Leitner, M. Baltrun, K. R. Fisher, H. Kopacka, K. Wurst, L. J. Daumann, D. Munz and S. Hohloch, *Inorg. Chem.*, 2021, **60**, 15421–15434.

28 S. Guo, H. Sivaram, D. Yuan and H. V. Huynh, *Organometallics*, 2013, **32**, 3685–3696.

29 H. Sivaram, J. Tan and H. V. Huynh, *Organometallics*, 2012, **31**, 5875–5883.

30 Q. Teng and H. V. Huynh, *Dalton Trans.*, 2017, **46**, 614–627.

31 (*a*) F. Buß, P. Mehlmann, C. Mück-Lichtenfeld, K. Bergander and F. Dielmann, *J. Am. Chem. Soc.*, 2016, **138**, 1840–1843; (*b*) F. Buß, M. B. Röthel, J. A. Werra, P. Rotering, L. F. B. Wilm, C. G. Daniliuc, P. Löwe and F. Dielmann, *Chem. – Eur. J.*, 2022, **28**, e202104021; (*c*) P. Mehlmann and F. Dielmann, *Chem. – Eur. J.*, 2019, **25**, 2352–2357; (*d*) P. Mehlmann, C. Mück-Lichtenfeld, T. T. Y. Tan and F. Dielmann, *Chem. – Eur. J.*, 2017, **23**, 5929–5933; (*e*) M. A. Wünsche, P. Mehlmann, T. Witteler, F. Buß, P. Rathmann and F. Dielmann, *Angew. Chem., Int. Ed.*, 2015, **54**, 11857–11860.

32 D. Menia, M. Pittracher, H. Kopacka, K. Wurst, F. R. Neururer, D. Leitner, S. Hohloch, M. Podewitz and B. Bildstein, *Organometallics*, 2023, **42**, 377–383.

33 R. Büssing, B. Karge, P. Lippmann, P. G. Jones, M. Brönstrup and I. Ott, *ChemMedChem*, 2021, **16**, 3402–3409.

34 (*a*) J. L. Hickey, R. A. Ruhayel, P. J. Barnard, M. V. Baker, S. J. Berners-Price and A. Filipovska, *J. Am. Chem. Soc.*, 2008, **130**, 12570–12571; (*b*) P. J. Barnard, M. V. Baker, S. J. Berners-Price and D. A. Day, *J. Inorg. Biochem.*, 2004, **98**, 1642–1647; (*c*) R. Rubbiani, S. Can, I. Kitanovic, H. Alborzinia, M. Stefanopoulou, M. Kokoschka, S. Mönchgesang, W. S. Sheldrick, S. Wölfl and I. Ott, *J. Med. Chem.*, 2011, **54**, 8646–8657; (*d*) R. Rubbiani, I. Kitanovic, H. Alborzinia, S. Can, A. Kitanovic, L. A. Onambele, M. Stefanopoulou, Y. Geldmacher, W. S. Sheldrick, G. Wolber, A. Prokop, S. Wölfl and I. Ott, *J. Med. Chem.*, 2010, **53**, 8608–8618.

35 (*a*) G. Moreno-Alcántar, P. Picchetti and A. Casini, *Angew. Chem., Int. Ed.*, 2023, **62**, e202218000; (*b*) E. Ansari, R. Kumar and A. Ratnam, *Dalton Trans.*, 2025, **54**, 7553–7601.

36 (*a*) J. T. Chantson, M. V. V. Falzacappa, S. Crovella and N. Metzler-Nolte, *J. Organomet. Chem.*, 2005, **690**, 4564–4572; (*b*) Y. Lin, G. Scalese, C. A. Bulman, R. Vinck, O. Blacque, M. Paulino, A. Ballesteros-Casallas, L. Pérez Díaz, G. Salinas, M. Mitreva, T. Weil, K. Cariou, J. A. Sakanari, D. Gambino and G. Gasser, *ACS Infect. Dis.*, 2024, **10**, 938–950.

37 (*a*) I. Ott, *Coord. Chem. Rev.*, 2009, **253**, 1670–1681; (*b*) M. Mora, M. C. Gimeno and R. Visbal, *Chem. Soc. Rev.*, 2019, **48**, 447–462; (*c*) Y. Lu, X. Ma, X. Chang, Z. Liang, L. Lv, M. Shan, Q. Lu, Z. Wen, R. Gust and W. Liu, *Chem. Soc. Rev.*, 2022, **51**, 5518–5556; (*d*) E. Schlegel, Z. Papadopoulos, N. Montesdeoca, V. A. Voloshkin, S. P. Nolan, S. A. Hahn, T. Scattolin and J. Karges, *ACS Med. Chem. Lett.*, 2025, **16**, 856–864; (*e*) A. Steinbrueck, M. L. Reback, C. Rumancev, D. Siegmund, J. Garrevoet, G. Falkenberg, A. Rosenhahn, A. Prokop and N. Metzler-Nolte, *Chem. – Eur. J.*, 2025, **31**, e202404147; (*f*) J. Weaver, S. Gaillard, C. Toye, S. Macpherson, S. P. Nolan and A. Riches, *Chem. – Eur. J.*, 2011, **17**, 6620–6624;

 This journal is © The Royal Society of Chemistry 2026

Open Access Article. Published on 17 December 2025. Downloaded on 6/10/2026 11:02:15 PM. This article is licensed under a Creative Commons Attribution 3.0 Unported Licence.

(*g*) D. Menia, H. Kopacka, K. Wurst, T. Müller, P. Lippmann, I. Ott and B. Bildstein, *Eur. J. Inorg. Chem.*, 2021, **2021**, 2784–2786.

38 J. Mellin, C. Bruhn, I. V. Esarev, I. Ott and U. Siemeling, *Z. Anorg. Allg. Chem.*, 2025, **651**, e202500124.

39 (*a*) M. B. Harbut, C. Vilchèze, X. Luo, M. E. Hensler, H. Guo, B. Yang, A. K. Chatterjee, V. Nizet, W. R. Jacobs, P. G. Schultz and F. Wang, *Proc. Natl. Acad. Sci. U. S. A.*, 2015, **112**, 4453–4458; (*b*) Y. Liu, Y. Lu, Z. Xu, X. Ma, X. Chen and W. Liu, *Drug Discovery Today*, 2022, **27**, 1961–1973; (*c*) C. Schmidt, B. Karge, R. Misgeld, A. Prokop, R. Franke, M. Brönstrup and I. Ott, *Chem. – Eur. J.*, 2017, **23**, 1869–1880.

40 S. Vanicek, H. Kopacka, K. Wurst, S. Vergeiner, S. Kankowski, J. Schur, B. Bildstein and I. Ott, *Dalton Trans.*, 2016, **45**, 1345–1348.

41 (*a*) J. P. Perdew, *Phys. Rev. B:Condens. Matter Mater. Phys.*, 1986, **33**, 8822–8824; (*b*) A. D. Becke, *Phys. Rev. A: Gen. Phys.*, 1988, **38**, 3098–3100; (*c*) F. Weigend and R. Ahlrichs, *Phys. Chem. Chem. Phys.*, 2005, **7**, 3297–3305; (*d*) S. Grimme, S. Ehrlich and L. Goerigk, *J. Comput. Chem.*, 2011, **32**, 1456–1465; (*e*) A. Schäfer, A. Klamt, D. Sattel, J. C. W. Lohrenz and F. Eckert, *Phys. Chem. Chem. Phys.*, 2000, **2**, 2187–2193; (*f*) A. Klamt and G. Schüürmann, *J. Chem. Soc., Perkin Trans. 2*, 1993, 799–805; (*g*) C. Adamo and V. Barone, *J. Chem. Phys.*, 1999, **110**, 6158–6170; (*h*) S. G. Balasubramani, G. P. Chen, S. Coriani, M. Diedenhofen, M. S. Frank, Y. J. Franzke, F. Furche, R. Grotjahn, M. E. Harding, C. Hättig, A. Hellweg, B. Helmich-Paris, C. Holzer, U. Huniar, M. Kaupp, A. Marefat Khah, S. Karbalaei Khani, T. Müller, F. Mack, B. D. Nguyen, S. M. Parker, E. Perlt, D. Rappoport, K. Reiter, S. Roy, M. Rückert, G. Schmitz, M. Sierka, E. Tapavicza, D. P. Tew, C. van Wüllen, V. K. Voora, F. Weigend, A. Wodyński and J. M. Yu, *J. Chem. Phys.*, 2020, **152**, 184107; (*i*) V. N. Staroverov, G. E. Scuseria, J. Tao and J. P. Perdew, *J. Chem. Phys.*, 2003, **119**, 12129–12137; (*j*) J. Tao, J. P. Perdew, V. N. Staroverov and G. E. Scuseria, *Phys. Rev. Lett.*, 2003, **91**, 146401; (*k*) E. Caldeweyher, S. Ehlert, A. Hansen, H. Neugebauer, S. Spicher, C. Bannwarth and S. Grimme, *J. Chem. Phys.*, 2019, **150**, 154122; (*l*) D. J. Nelson and S. P. Nolan, *Chem. Soc. Rev.*, 2013, **42**, 6723–6753; (*m*) J. Mathew and C. H. Suresh, *Inorg. Chem.*, 2010, **49**, 4665–4669; (*n*) A. D. Becke, *J. Chem. Phys.*, 1993, **98**, 5648–5652; (*o*) R. Krishnan, J. S. Binkley, R. Seeger and J. A. Pople, *J. Chem. Phys.*, 1980, **72**, 650–654; (*p*) T. Clark, J. Chandrasekhar, G. W. Spitznagel and P. V. R. Schleyer, *J. Comput. Chem.*, 1983, **4**, 294–301; (*q*) K. Raghavachari and G. W. Trucks, *J. Chem. Phys.*, 1989, **91**, 1062–1065; (*r*) L. Schrödinger and W. DeLano, *PyMOL*, 2020; (*s*) W. Humphrey, A. Dalke and K. Schulten, *J. Mol. Graphics*, 1996, **14**, 33–38.

42 (*a*) CCDC 2314980: Experimental Crystal Structure Determination, 2025, DOI: 10.5517/ccdc.csd.cc2hpxsx; (*b*) CCDC 2314979: Experimental Crystal Structure Determination, 2025, DOI: 10.5517/ccdc.csd.cc2hpxrw; (*c*) CCDC 2476574: Experimental Crystal Structure Determination, 2025, DOI: 10.5517/ccdc.csd.cc2p42hf; (*d*) CCDC 2314982: Experimental Crystal Structure Determination, 2025, DOI: 10.5517/ccdc.csd.cc2hpxvz; (*e*) CCDC 2314981: Experimental Crystal Structure Determination, 2025, DOI: 10.5517/ccdc.csd.cc2hpxty; (*f*) CCDC 2314983: Experimental Crystal Structure Determination, 2025, DOI: 10.5517/ccdc.csd.cc2hpxw0; (*g*) CCDC 2314984: Experimental Crystal Structure Determination, 2025, DOI: 10.5517/ccdc.csd.cc2hpxx1.